CANCER IMMUNOLOGY

Vitamin D regulates microbiome-dependent cancer immunity

Evangelos Giampazolias[1,2]*, Mariana Pereira da Costa[1]†, Khiem C. Lam[3]†, Kok Haw Jonathan Lim[1,4]†‡, Ana Cardoso[1]†, Cécile Piot[1]†, Probir Chakravarty[5], Sonja Blasche[6], Swara Patel[2], Adi Biram[1], Tomas Castro-Dopico[1], Michael D. Buck[1], Richard R. Rodrigues[7,8], Gry Juul Poulsen[9], Susana A. Palma-Duran[10]§, Neil C. Rogers[1], Maria A. Koufaki[11], Carlos M. Minutti[1]¶, Pengbo Wang[2], Alexander Vdovin[2], Bruno Frederico[1]#, Eleanor Childs[1], Sonia Lee[1], Ben Simpson[12], Andrea Iseppon[13]**, Sara Omenetti[13]††, Gavin Kelly[5], Robert Goldstone[5], Emma Nye[14], Alejandro Suárez-Bonnet[14,15], Simon L. Priestnall[14,15], James I. MacRae[10], Santiago Zelenay[11], Kiran Raosaheb Patil[6], Kevin Litchfield[12], James C. Lee[16,17], Tine Jess[9], Romina S. Goldszmid[3], Caetano Reis e Sousa[1]*

A role for vitamin D in immune modulation and in cancer has been suggested. In this work, we report that mice with increased availability of vitamin D display greater immune-dependent resistance to transplantable cancers and augmented responses to checkpoint blockade immunotherapies. Similarly, in humans, vitamin D–induced genes correlate with improved responses to immune checkpoint inhibitor treatment as well as with immunity to cancer and increased overall survival. In mice, resistance is attributable to the activity of vitamin D on intestinal epithelial cells, which alters microbiome composition in favor of *Bacteroides fragilis*, which positively regulates cancer immunity. Our findings indicate a previously unappreciated connection between vitamin D, microbial commensal communities, and immune responses to cancer. Collectively, they highlight vitamin D levels as a potential determinant of cancer immunity and immunotherapy success.

The micronutrient vitamin D has an important role in immune modulation and in shaping commensal microbial communities (*1*–*6*). Vitamin D has also been studied for its potential role in cancer, with reports showing that it can decrease cancer cell proliferation, promote apoptosis, reduce angiogenesis (*7*–*9*), and dampen the protumorigenic activity of cancer-associated fibroblasts (*10*, *11*). In some but not all studies, higher blood levels or increased dietary intake of vitamin D have been correlated with a lower incidence of colorectal, breast, prostate, and pancreatic tumors and/or decreased cancer mortality (*12*–*21*). However, to what extent the activity of vitamin D affects cancer development, and whether this involves the immune system and/or the microbiome, remains unclear.

Vitamin D (calciferol) is a term that includes both vitamin D_3 (cholecalciferol) and vitamin D_2 (ergocalciferol) forms of the vitamin. Vitamin D_3 is derived from animal-sourced foods or is produced by the skin in response to ultraviolet radiation, whereas vitamin D_2 is derived from plants and fungi (*22*). Irrespective of source, both vitamin D_2 and D_3 are converted in the liver and other tissues to 25-hydroxyvitamin D (25-OHD), the main circulating form of vitamin D (*22*). 25-OHD is then converted primarily in the kidney to 1,25-dihydroxy-vitamin D [1,25-$(OH)_2$D], which can bind to the vitamin D receptor (VDR) to regulate the expression of vitamin D–responsive genes (*22*). Notably, vitamin D and its 25-OHD and 1,25-$(OH)_2$D metabolites (collectively called VitD henceforth) are bound by the blood carrier protein group-specific component (Gc) globulin, also known as the vitamin D binding protein. Gc has a domain at its N terminus with high affinity for 25-OHD and lower affinity for its precursor calciferol and for 1,25-$(OH)_2$D (*23*, *24*). Gc binding sequesters VitD, principally 25-OHD, away from tissues, acting as a blood reservoir (*24*, *25*). Despite the prominent role of VitD in calcium homeostasis, $Gc^{-/-}$ mice (and a rare human patient displaying biallelic *GC* loss) do not display bone abnormalities (e.g., rickets or osteomalacia) associated with VitD deficiency (*24*, *26*). Rather, animals lacking the Gc globulin display low levels of VitD in the blood, which results in more rapid and profound tissue responses to VitD at the expense of low buffering capacity (*24*).

Cross-presentation of tumor antigens by type 1 conventional dendritic cells (cDC1s) is critical for generating anticancer $CD8^+$ T cells (*27*, *28*). In mice and humans, cDC1s express DNGR-1 (also known as CLEC9A), a receptor that binds to F-actin exposed by dying cells and promotes cross-presentation of antigens within the corpses (*29*, *30*). Previously, we had shown that secreted gelsolin (sGSN), an extracellular protein that circulates in the plasma and is secreted by tumor cells, severs F-actin and blocks DNGR-1 ligand binding, dampening anticancer immunity and the efficacy of immunogenic anticancer therapies (*31*, *32*). Notably, Gc globulin has a C-terminal actin-binding domain and functions as an actin scavenging protein in partnership with sGSN—a role that is independent of VitD buffering (*33*). We therefore set out to test whether, like sGSN, Gc acts as a barrier to anticancer $CD8^+$ T cell responses. We show that this is the case but that it is not attributable to actin scavenging but rather to Gc regulation of VitD availability. We uncover a complex interplay whereby increased VitD levels promote responses from intestinal epithelial cells (IECs) that modulate the gut microbiome, which in turn acts to potentiate anticancer immunity. Notably, the effect of increased VitD availability on immune-mediated resistance to cancer can be transferred in dominant fashion to microbiota-replete mice by transplantation of fecal matter or oral inoculation with the bacterium *Bacteroides fragilis*, provided that dietary vitamin D intake is maintained. In humans, we show that vitamin D levels correlate with lower cancer incidence

[1]Immunobiology Laboratory, The Francis Crick Institute, London NW1 1AT, UK. [2]Cancer Immunosurveillance Group, Cancer Research UK Manchester Institute, The University of Manchester, Manchester M20 4BX, UK. [3]Inflammatory Cell Dynamics Section, Laboratory of Integrative Cancer Immunology (LICI), Center for Cancer Research (CCR), National Cancer Institute (NCI), Bethesda, MD 20892, USA. [4]Department of Immunology and Inflammation, Imperial College London, London SW7 2AZ, UK. [5]Bioinformatics and Biostatistics STP, The Francis Crick Institute, London NW1 1AT, UK. [6]MRC Toxicology Unit, University of Cambridge, Cambridge CB2 1QR, UK. [7]Basic Science Program, Frederick National Laboratory for Cancer Research, Frederick, MD 21701, USA. [8]Microbiome and Genetics Core, LICI, CCR, NCI, Bethesda, MD 20892, USA. [9]National Center of Excellence for Molecular Prediction of Inflammatory Bowel Disease, PREDICT, Faculty of Medicine, Aalborg University, Department of Gastroenterology and Hepatology, Aalborg University Hospital, A DK-2450 Copenhagen, Denmark. [10]Metabolomics STP, The Francis Crick Institute, London NW1 1AT, UK. [11]Cancer Inflammation and Immunity Group, Cancer Research UK Manchester Institute, The University of Manchester, Manchester M20 4BX, UK. [12]Tumor Immunogenomics and Immunosurveillance (TIGI) Lab, UCL Cancer Institute, London WC1E 6DD, UK. [13]AhRimmunity Laboratory, The Francis Crick Institute, London NW1 1AT, UK. [14]Experimental Histopathology, The Francis Crick Institute, London NW1 1AT, UK. [15]Department of Pathobiology and Population Sciences, The Royal Veterinary College, North Mimms, Hatfield, Hertfordshire AL9 7TA, UK. [16]Genetic Mechanisms of Disease Laboratory, The Francis Crick Institute, London NW1 1AT, UK. [17]Institute of Liver and Digestive Health, Division of Medicine, Royal Free Hospital, University College London, London NW3 2QG, UK.

***Corresponding author. Email: caetano@crick.ac.uk (C.R.e.S.); evangelos.giampazolias@cruk.manchester.ac.uk (E.G.)**

†These authors contributed equally to this work.

‡Present address: The Christie NHS Foundation Trust, Manchester M20 4BX, UK.

§Present address: Department of Food Science, Research Center in Food and Development A.C., La Victoria, Hermosillo, 83304, Mexico.

¶Present address: Immunoregulation Laboratory, Champalimaud Research, Champalimaud Centre for the Unknown, 1400-038 Lisbon, Portugal.

#Present address: The Discovery Centre, Cambridge Biomedical Campus, Cambridge CB2 0AA, UK.

**Present address: Catenion GmbH, Headquarters EU, 10178 Berlin, Germany.

††Present address: CancerTools.org, London E20 1JQ, UK.

and that hallmarks of VDR activity are associated with better disease outcomes in cancer patients and improved responses to checkpoint blockade immunotherapy. Overall, our data suggest that VitD can regulate the microbiome and anticancer immunity, with possible clinical and public health applications.

Gc-deficient mice display immune-dependent transmissible tumor resistance

We set out to test whether Gc, like sGSN, acts as a barrier to anticancer immunity. We used the transplantable 5555 Braf^{V600E} melanoma cell line, the growth of which is greatly attenuated in *sGsn*$^{-/-}$ mice (*31*), and examined its ability to grow in *Gc*$^{-/-}$ mice (*24*) versus *Gc*$^{+/+}$ littermate controls that were separated at weaning and housed in different cages. Gc-deficient mice (fully backcrossed to the C57BL/6J background) controlled the 5555 Braf^{V600E} melanoma cell line significantly better compared with Gc-sufficient littermate controls (Fig. 1A) and displayed greater intratumoral accumulation of total and activated CD4$^+$ and CD8$^+$ T cells (Fig. 1B). The relative resistance of *Gc*$^{-/-}$ mice to 5555 Braf^{V600E} melanoma was abrogated by antibody-mediated CD8$^+$ T cell depletion (Fig. 1C). Additionally, *Gc*$^{-/-}$ mice bearing 5555 Braf^{V600E} melanoma or MCA-205 fibrosarcoma tumors displayed greater responses to anti–PD-1 and anti–CTLA-4 checkpoint blockade immunotherapies compared with C57BL6/J wild-type (WT) mice (Fig. 1, D to F). Thus, like *sGsn*$^{-/-}$ mice, *Gc*$^{-/-}$ mice exhibit enhanced CD8$^+$ T cell–dependent resistance to transplantable tumors and superior responsiveness to checkpoint blockade immunotherapies.

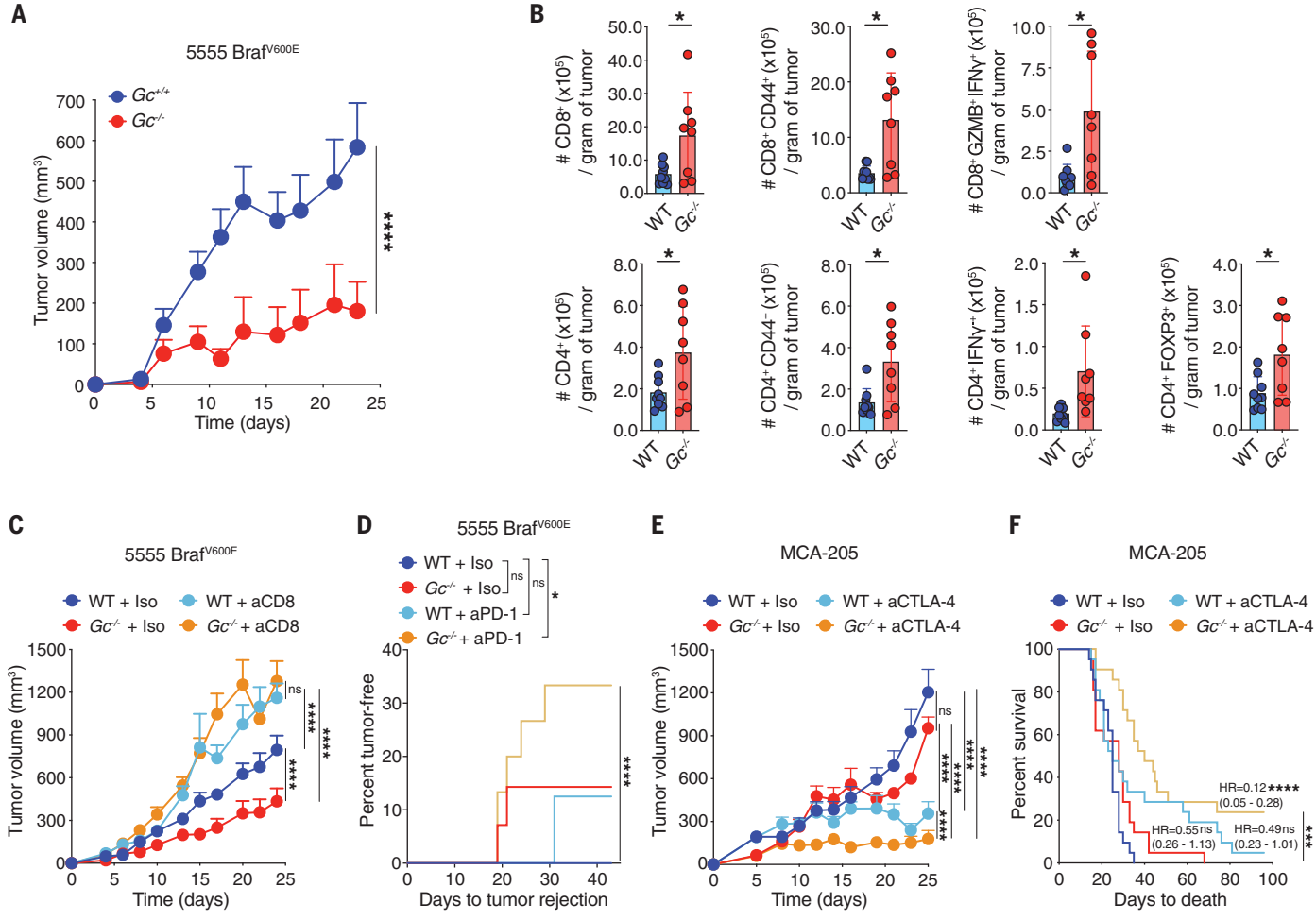

Fig. 1. Loss of Gc increases CD8$^+$ T cell–dependent tumor control and augments response to immunotherapy. (**A**) Growth profile of 0.2 × 10^6 5555 Braf^{V600E} cancer cells implanted in separately housed groups of *Gc*$^{-/-}$ mice (n = 8) and *Gc*$^{+/+}$ littermate control mice (n = 11). (**B**) Quantification of the indicated intratumoral immune cell populations in separately housed groups of WT C57BL/6J (n = 9) or *Gc*$^{-/-}$ (n = 8) mice at day 15 postinoculation with 5555 Braf^{V600E} cancer cells. Data are presented as number of cells per gram of tumor from two independent experiments. (**C**) Same as in (A), but mice received anti-CD8 antibody or isotype-matched control [300 μg intraperitoneally (i.p.) on days −3, 1, 4, 7, 10, 13, 16, 19, and 22]. WT C57BL/6J + isotype (n = 12), WT C57BL/6J + anti-CD8 (n = 12), *Gc*$^{-/-}$ + isotype (n = 14), and *Gc*$^{-/-}$ + anti-CD8 (n = 13). (**D**) Percent of 5555 Braf^{V600E} tumor rejection from two independent experiments in separately housed WT C57BL/6J or *Gc*$^{-/-}$ groups of mice that received anti–PD-1 monoclonal antibody or isotype-matched control (200 μg i.p. every 3 days from day 3 to day 18). WT + isotype (n = 15), WT + anti–PD-1 (n = 16), *Gc*$^{-/-}$ + isotype (n = 14), *Gc*$^{-/-}$ + anti–PD-1 (n = 15). (**E** and **F**) Separately housed WT C57BL/6J or *Gc*$^{-/-}$ groups of mice implanted with 0.5 × 10^6 MCA-205 and given isotype-matched control or anti–CTLA-4 (50 μg injected i.p. on days 6, 9, and 12). (E) Growth profile (n = 10 mice per group). (F) Survival (Kaplan-Meier) curves from two independent experiments (n = 21 mice per group). Data in (A), (C), and (E) are presented as tumor volumes (in cubic millimeters) + SEMs and are representative of two independent experiments. Tumor growth profiles [(A), (C), and (E)] were compared using Bonferroni-corrected two-way analysis of variance (ANOVA). Groups in (B) were compared using two-tailed unpaired t test with Welch's correction. Incidence of tumor rejection and survival (Kaplan-Meier) curves in (D) and (F) were compared using log-rank (Mantel-Cox) test for comparison of each group with WT C57BL/6J + isotype and log-rank for trend for comparison of all groups. In (F), hazard ratios (HRs) with 95% confidence intervals are shown in brackets, calculated as a ratio of each group/WT + isotype. *P < 0.05; ***P < 0.001; ****P < 0.0001; ns, not significant.

To control for possible differences in microbiota between $Gc^{-/-}$ mice and $Gc^{+/+}$ controls separated at weaning, we repeated the experiments in $Gc^{-/-}$ and $Gc^{+/+}$ littermates kept in the same cages. Notably, cohoused $Gc^{+/+}$ mice acquired the tumor resistance phenotype of their Gc-deficient littermates (Fig. 2A). Similarly, C57BL6/J WT mice (bred as an independent line) became more resistant to tumor challenge when cohoused with $Gc^{-/-}$ mice (fig. S1A). This transmissible tumor resistance was reversible, as $Gc^{+/+}$ littermate controls cohoused since birth with $Gc^{-/-}$ mice were less able to control tumors when separated for at least a month before tumor challenge (Fig. 1A and Fig. 2A). These data suggest that (i) $Gc^{-/-}$ and $Gc^{+/+}$ mice exhibit genotype-driven divergence in microbiota composition, which dictates their differential ability to control tumors, and (ii) the $Gc^{-/-}$-associated component of the microbiota that mediates tumor resistance can be transmitted in a dominant fashion to cohoused mice by coprophagy. Consistent with the latter, fecal transplant (FT) from $Gc^{-/-}$ donors into microbiota-replete C57BL/6 WT mice led to enhanced tumor control (Fig. 2B). Further, single administration of certain antibiotics (vancomycin, metronidazole, or neomycin) inhibited or decreased the ability of $Gc^{-/-}$ mice to control transplantable tumors (Fig. 2C and fig. S1B).

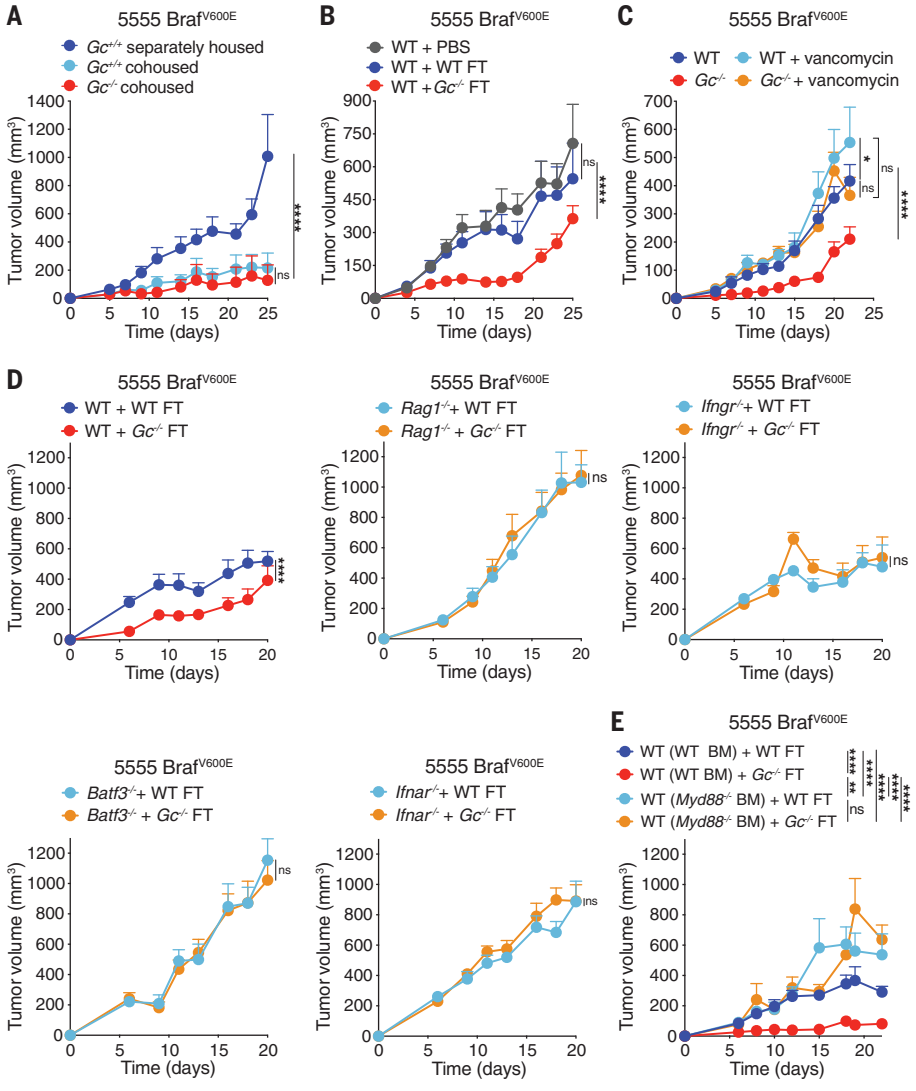

Fig. 2. FTs from $Gc^{-/-}$ mice increase anticancer immunity. (A to E) Growth profile of 0.2 × 10^6 5555 Braf^{V600E} cancer cells implanted into: (**A**) Separately housed $Gc^{+/+}$ (n = 12) and cohoused $Gc^{+/+}$ (n = 7) and $Gc^{-/-}$ (n = 6) groups of mice. (**B**) Separately housed groups of WT C57BL/6J mice (n = 10 per group) that received phosphate-buffered saline (PBS) orally or FT from WT or $Gc^{-/-}$ donors twice (days −14 and −12) before tumor inoculation (day 0). (**C**) Separately housed groups of WT C57BL/6J or $Gc^{-/-}$ mice that received or did not receive vancomycin (0.5 g/l) in the drinking water starting from 2 weeks before tumor inoculation. WT (n = 11), WT + vancomycin (n = 10), $Gc^{-/-}$ (n = 11), $Gc^{-/-}$ + vancomycin (n = 10). (**D** and **E**) The indicated separately housed groups of mice that received oral FT from WT C57BL/6J or $Gc^{-/-}$ donors twice (days −14 and −12) before tumor inoculation (day 0). (D) WT (n = 11 per group), $Rag1^{-/-}$ (n = 9 per group), $Ifngr1^{-/-}$ (n = 10 per group), $Batf3^{-/-}$ (n = 10), and $Ifnar^{-/-}$ (n = 10 per group) mice. (E) Irradiated CD45.1 WT mice reconstituted using bone marrow (BM) from CD45.2 WT or $Myd88^{-/-}$ donors. WT (WT BM) + WT FT (n = 11), WT (WT BM) + $Gc^{-/-}$ FT (n = 12), WT ($Myd88^{-/-}$ BM) + WT FT (n = 10), WT ($Myd88^{-/-}$ BM) $Gc^{-/-}$ FT (n = 10). Data in (A) to (E) are presented as tumor volumes + SEMs and are representative of two independent experiments. Tumor growth profiles were compared using Bonferroni-corrected two-way ANOVA. *P < 0.05; **P < 0.01; ***P < 0.001; ****P < 0.0001; ns, not significant.

The antitumor effect of the intestinal microbiome of $Gc^{-/-}$ mice was not accompanied by obvious signs of gut inflammation or histological changes to the intestinal barrier (fig. S1C). The extent of gut-associated lymphoid tissue, gut permeability, total leukocyte numbers, and immune cell composition of intestinal lamina propria were all grossly similar between WT and $Gc^{-/-}$ mice, except for a decrease in the frequency of interleukin-17 (IL-17)–producing CD4$^+$ T cells in the small intestine and of total CD4$^+$ T cells and regulatory T cells in the colon of Gc-deficient hosts (fig. S1, D to I). Moreover, FT of $Gc^{-/-}$ fecal matter into WT mice did not increase the severity of dextran sodium sulfate (DSS)–induced colitis (fig. S2, A to D). Collectively, these data suggest that the commensal organisms present in the intestine of Gc-deficient mice do not markedly alter barrier function or mucosal immunity, either at steady state or after induction of intestinal inflammation.

To confirm that the transmissible resistance to transplantable tumors was immune dependent and to dissect the pathways involved, we tested different immune-deficient strains (Fig. 2D and fig. S3A). FT from $Gc^{-/-}$ donors into mice deficient in T and B cells ($Rag1^{-/-}$) or interferon-γ (IFN-γ) receptor ($Ifngr^{-/-}$) did not confer enhanced protection to subsequent tumor challenge (Fig. 2D). Similarly, mice deficient in CD8$^+$ T cells and major histocompatibility complex (MHC) class I presentation ($Tap1^{-/-}$) or cDC1 ($Batf3^{-/-}$) did not display enhanced control of transplantable tumors when given $Gc^{-/-}$ fecal matter (Fig. 2D and fig. S3A). Global deletion of type I IFN receptor (IFNAR) or MyD88 [an adaptor molecule that operates downstream of IL-1 family receptors and Toll-like receptors (TLRs)] also diminished tumor resistance conferred by $Gc^{-/-}$ FT (Fig. 2D and fig. S3B). Using bone marrow radiation chimeras, MyD88 expression in the hematopoietic compartment was found to be necessary and sufficient for enhanced tumor control (Fig. 2E and fig. S3C). By contrast, the DNA sensor cGAS and the TLR adaptor molecule TRIF were dispensable for increased tumor resistance after $Gc^{-/-}$ FT administration (fig. S3B). Collectively, these data indicate a key role for innate and adaptive immunity in the

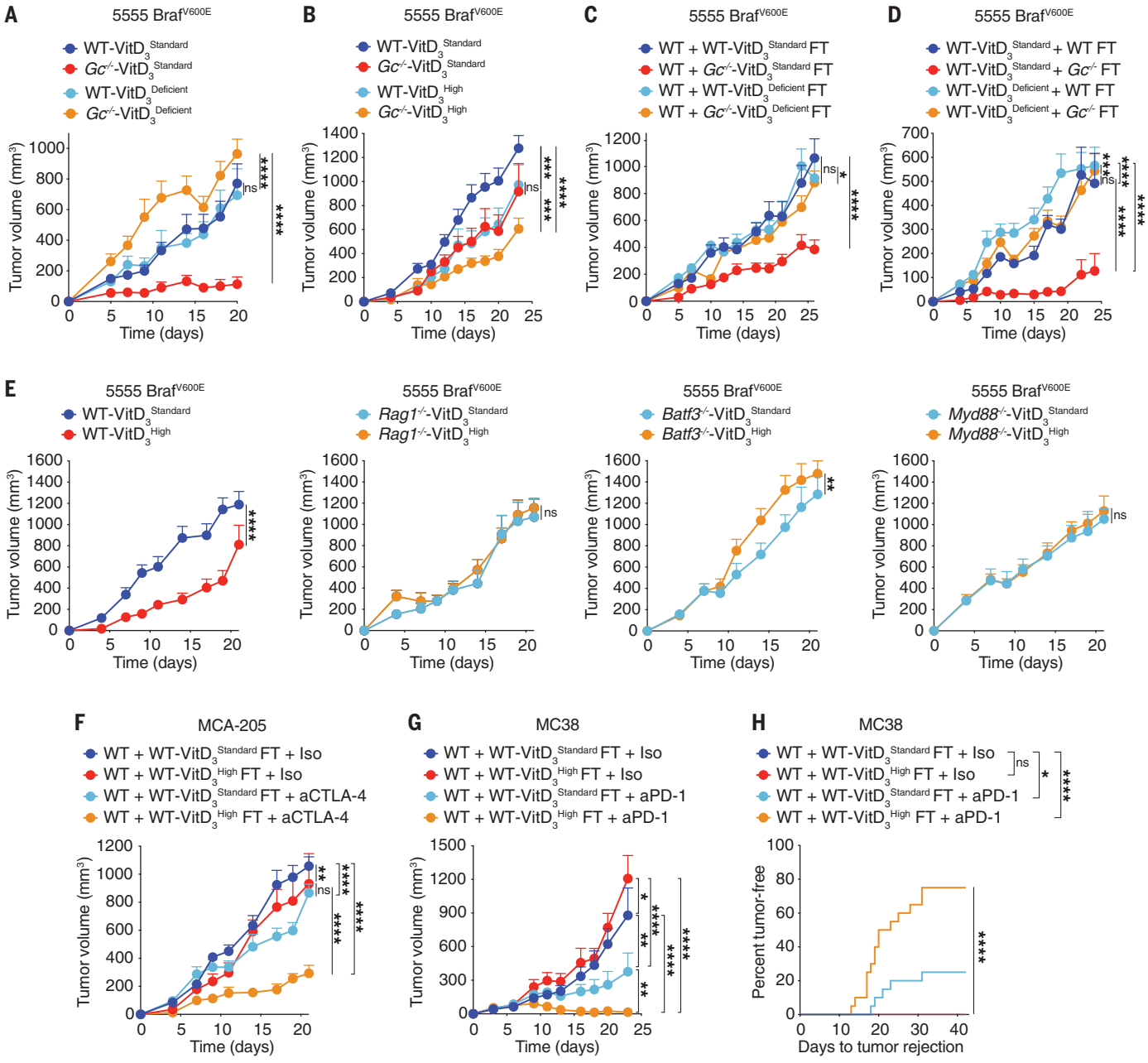

Fig. 3. Loss of Gc increases VitD-dependent anticancer immunity by altering the gut microbiome. (A to E) Growth profile of 0.2 × 10^6 5555 Braf^{V600E} cancer cells implanted into: (**A** and **B**) WT C57BL/6J or *Gc*$^{-/-}$ mice that were fed a $VitD_3$ standard (2 IU/g), deficient (0 IU/g), or high (10 IU/g) diet starting from 3.5 weeks before tumor inoculation. (A) WT + $VitD_3^{Standard}$ (n = 8), WT + $VitD_3^{Deficient}$ (n = 9), *Gc*$^{-/-}$ + $VitD_3^{Standard}$ (n = 8), *Gc*$^{-/-}$ + $VitD_3^{Deficient}$ (n = 9). (B) WT + $VitD_3^{Standard}$ (n = 12), WT + $VitD_3^{High}$ (n = 13), *Gc*$^{-/-}$ + $VitD_3^{Standard}$ (n = 12), *Gc*$^{-/-}$ + $VitD_3^{High}$ (n = 13). (**C**) WT C57BL/6J (n = 10 per group) that received (on days −14 and −12 before tumor inoculation) FT from WT C57BL/6J or *Gc*$^{-/-}$ donors that had been fed with $VitD_3$ standard or deficient diet. (**D**) WT C57BL/6J mice that were fed a $VitD_3$ standard or deficient diet starting 3.5 weeks before FT (on days −14 and −12 before tumor inoculation) with fecal matter from WT C57BL/6J or *Gc*$^{-/-}$ donors. WT-$VitD_3^{Standard}$ + WT FT (n = 7), WT-$VitD_3^{Standard}$ + WT *Gc*$^{-/-}$ (n = 10), WT-$VitD_3^{Deficient}$ + WT FT (n = 10), WT-$VitD_3^{Deficient}$ + WT *Gc*$^{-/-}$ FT (n = 10). (**E**) WT C57BL/6J, *Rag1*$^{-/-}$, *Batf3*$^{-/-}$, or *Myd88*$^{-/-}$ mice (n = 10 per group) that were fed with $VitD_3$ standard or high diet starting from 3.5 weeks before tumor inoculation. (**F**) Growth profile of 0.5 × 10^6 MCA-205 cancer cells implanted into WT C57BL/6J mice (n = 10 per group) that received (on days −14 and −12 before tumor inoculation) FT from WT C57BL/6J donors that were fed with $VitD_3$ standard or high diet. Mice were treated i.p. with 50 μg of isotype-matched control or anti–CTLA-4 antibody on days 6, 9, and 12. (**G** and **H**) Separately housed groups of WT C57BL/6J mice that received (on days −14 and −12 before tumor inoculation) FT from WT C57BL/6J donors that had been fed with $VitD_3$ standard or high diet were implanted with 0.5 × 10^6 MC38 cells (day 0). Mice were treated i.p. with 200 μg of isotype-matched control or anti–PD-1 monoclonal antibody every 3 days from day 3 to day 12. (G) Growth profile (n = 10 mice per group). (H) Percent tumor rejection from two independent experiments (n = 20 mice per group). Data in (A) to (G) are presented as tumor volumes + SEMs and are representative of two independent experiments. Tumor growth profiles [(A) to (G)] were compared using Bonferroni-corrected two-way ANOVA. Incidence of tumor rejection in (H) were compared using log-rank (Mantel-Cox) test for comparison of each group with WT C57BL/6J + isotype and log-rank for trend for comparison of all groups. *P < 0.05; **P < 0.01; ***P < 0.001; ****P < 0.0001; ns, not significant.

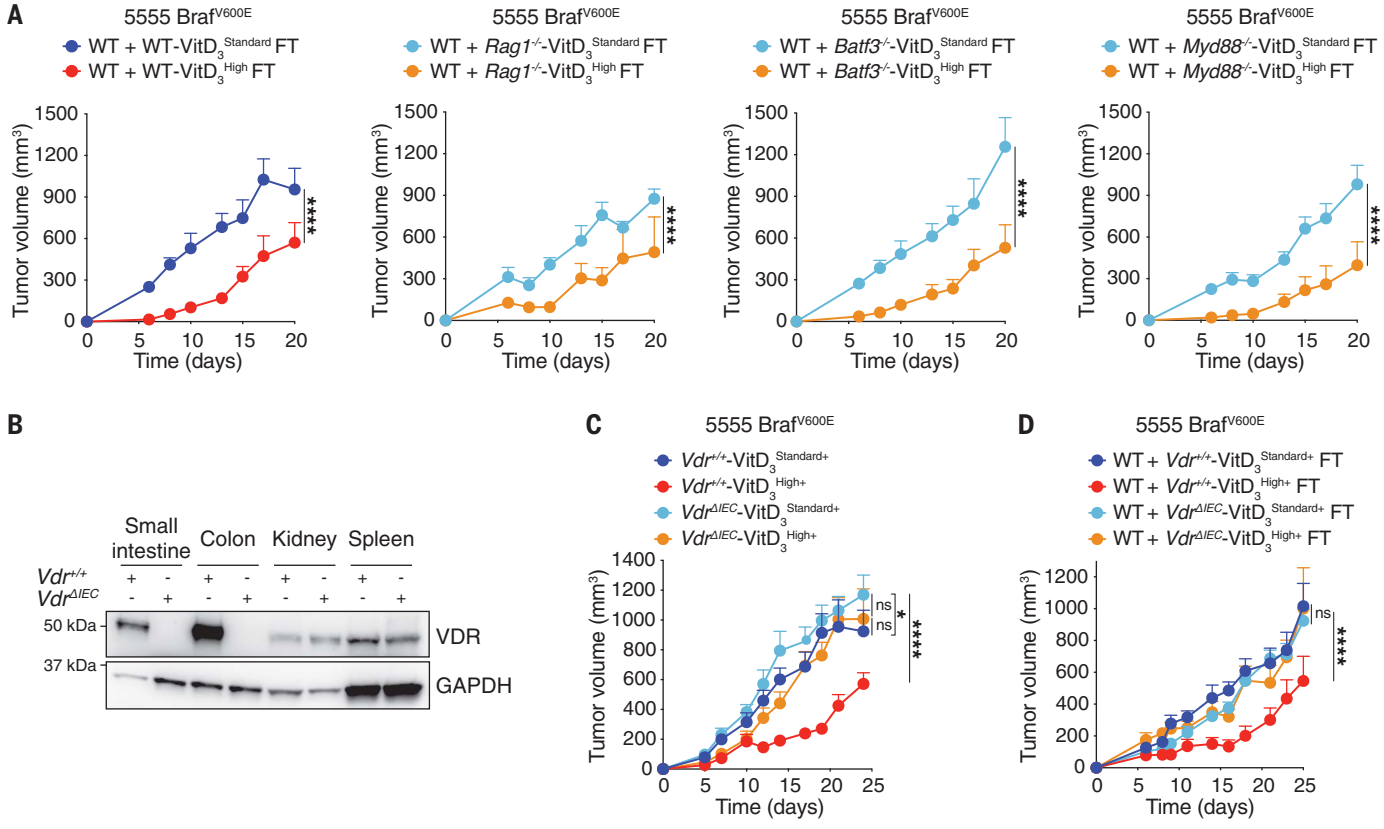

Fig. 4. VitD acts through VDR in the gut epithelium to alter the gut microbiome and permit tumor control. (A, C, and D) Growth profile of 0.2×10^6 5555 Braf^{V600E} cancer cells implanted into: (**A**) WT C57BL/6J mice that received (on days −14 and −12 before tumor inoculation) FT from WT C57BL/6J, *Rag1*$^{-/-}$, *Batf3*$^{-/-}$, or *Myd88*$^{-/-}$ donors that had been fed for 3.5 weeks on a $VitD_3$ standard or $VitD_3$ high diet. WT + WT-$VitD_3^{Standard}$ FT (n = 10), WT + WT-$VitD_3^{High}$ FT (n = 10), WT + *Rag1*$^{-/-}$-$VitD_3^{Standard}$ FT (n = 10), WT + *Rag1*$^{-/-}$-$VitD_3^{High}$ FT (n = 9), WT + *Batf3*$^{-/-}$-$VitD_3^{Standard}$ FT (n = 11), WT + *Batf3*$^{-/-}$-$VitD_3^{High}$ FT (n = 11), WT + *Myd88*$^{-/-}$-$VitD_3^{Standard}$ FT (n = 9), WT + *Myd88*$^{-/-}$-$VitD_3^{High}$ FT (n = 9). (**B**) Lysates from the indicated mouse tissues of *Vdr*$^{+/+}$ and *Vdr*$^{\Delta IEC}$ mice immunoblotted for VDR and glyceraldehyde-3-phosphate dehydrogenase (GAPDH). (**C**) *Vdr*$^{+/+}$ or *Vdr*$^{\Delta IEC}$ mice kept on a $VitD_3$ standard$^+$ (2 IU/g) diet complemented with 2% calcium, 1.25% phosphorus, and 20% lactose were then maintained on the same diet or switched to a $VitD_3$ high$^+$ (10 IU/g) diet (similarly complemented with 2% calcium, 1.25% phosphorus, and 20% lactose) from 3.5 weeks before tumor inoculation. *Vdr*$^{+/+}$-$VitD_3^{Standard+}$ (n = 12), *Vdr*$^{+/+}$-$VitD_3^{High+}$ (n = 11), *Vdr*$^{\Delta IEC}$-$VitD_3^{Standard+}$ (n = 15), *Vdr*$^{\Delta IEC}$-$VitD_3^{High+}$ (n = 15). (**D**) WT C57BL/6J mice (n = 10 per group) received (on days −14 and −12 before tumor inoculation) FT from the groups in (C)—i.e., *Vdr*$^{+/+}$ or *Vdr*$^{\Delta IEC}$ donors that were fed with $VitD_3$ standard$^+$ or $VitD_3$ high$^+$ diet. Data in (A), (C), and (D) are presented as tumor volumes + SEMs and are representative of two independent experiments. Tumor growth profiles [(A), (C), and (D)] were compared using Bonferroni-corrected two-way ANOVA. *$P < 0.05$; ****$P < 0.0001$; ns, not significant.

enhanced tumor resistance conferred by *Gc*$^{-/-}$ microbiota.

Vitamin D availability determines transmissible tumor resistance in mice

Because mice deficient in sGSN do not transfer tumor resistance to cohoused WT mice (*31*), we hypothesized that a deficiency in actin scavenging was not responsible for the enhanced tumor resistance in *Gc*$^{-/-}$ mice. As expected (*24*), *Gc*$^{-/-}$ mice displayed lower levels of vitamin D_3 and 25-OHD_3 in plasma, indicative of VitD redistribution to tissues (fig. S4A). The main vitamin D in mouse chow is cholecalciferol ($VitD_3$). To test whether Gc deficiency enhances tumor resistance in a VitD-dependent manner, WT and *Gc*$^{-/-}$ mice were put on a $VitD_3$-deficient diet for ~4 weeks to deplete their VitD reservoirs (fig. S4A). This completely abrogated the enhanced ability of *Gc*$^{-/-}$ mice to resist tumors (Fig. 3A). In the converse experiment, increased dietary $VitD_3$ supplementation led to elevated total VitD serum levels (fig. S4A) and decreased tumor growth in WT mice to the point that they became comparable to Gc-deficient animals fed with standard $VitD_3$ chow (Fig. 3B). The latter strain displayed even greater tumor resistance when placed on a high-$VitD_3$ diet (Fig. 3B). Collectively, these data suggest that enhanced VitD availability, induced by loss of Gc and/or by dietary $VitD_3$ supplementation, promotes increased resistance to transplantable tumors in mice.

We next assessed whether, as for Gc deficiency, dietary $VitD_3$ supplementation increases tumor resistance through the microbiota. Consistent with that notion, a high-$VitD_3$ diet did not increase the ability of germ-free mice to resist tumors (fig. S4B). Further, the capacity to transmit increased tumor resistance to WT mice was abrogated when fecal material was derived from *Gc*$^{-/-}$ mice that had been placed on a $VitD_3$-deficient diet (Fig. 3C). Conversely, increasing dietary $VitD_3$ in WT mice conferred their fecal matter the ability to transmit tumor control, which was prevented by treatment with vancomycin (fig. S4, C and D). FT from WT mice that were fed with a high-$VitD_3$ diet transferred tumor resistance to C576BL/6 mice from three different sources that were imported and housed in geographically distinct animal units (fig. S4E). Finally, we established that VitD availability in the recipient mice was also necessary for the beneficial antitumor effects of FT from *Gc*$^{-/-}$ donors. Enhanced resistance to tumors was prevented if the FT recipients were placed on a $VitD_3$-deficient diet (Fig. 3D).

In parallel, we tested whether manipulation of dietary $VitD_3$ affected tumor growth by modulating cancer immunity. Like Gc-deficient hosts

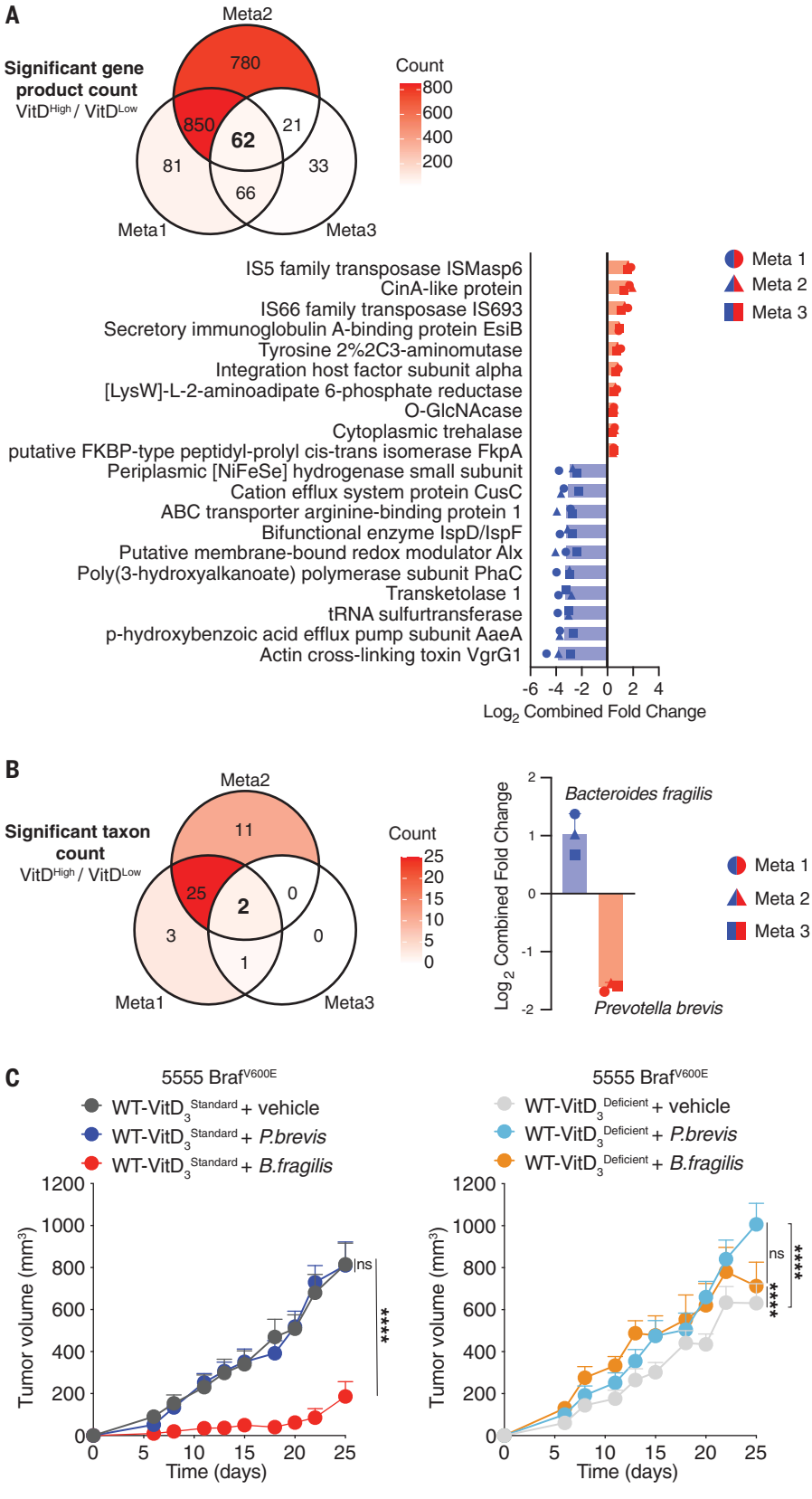

Fig. 5. *B. fragilis* promotes tumor resistance in a VitD-dependent manner. (**A** and **B**) Meta-analysis of metagenomic data to determine common features in microbial gene products (top 20/62 features in each direction shown) (A) and last known taxon associated with differences in VitD availability (B). Fecal samples were sequenced from WT or $Gc^{-/-}$ mice that had been fed with $VitD_3$ standard (2 IU/g), deficient (0 IU/g), or high (10 IU/g) diet for 3.5 weeks. Comparison is of mice with high VitD availability [WT + $VitD_3^{High}$ (n = 13), $Gc^{-/-}$ + $VitD_3^{Standard}$ (n = 20), $Gc^{-/-}$ + $VitD_3^{High}$ (n = 13)] versus mice with normal or low VitD availability [WT + $VitD_3^{Standard}$ (n = 22), WT + $VitD_3^{Deficient}$ (n = 10), $Gc^{-/-}$ + $VitD_3^{Deficient}$ (n = 10)]. In (A) and (B), count of significant features indicated in the Venn diagram and shown by color scale (top) and ranked bar plots (bottom) show common features across three meta-analyses, as indicated. (**C**) Growth profile of 0.2×10^6 5555 $Braf^{V600E}$ cancer cells implanted into separately housed WT C57BL/6 groups of mice (n = 10 per group) fed with $VitD_3$ standard (left) or deficient diet (right) starting 3.5 weeks before receiving *B. fragilis*, *P. brevis*, or vehicle. Mice received 10^9 *B. fragilis* or *P. brevis* by oral gavage on days −14, −12, and −10 before tumor inoculation. Data in (A) and (B) are presented as average $\log_2$ median fold change from three meta-analyses of data from two independent experiments. Data in (C) are presented as tumor volumes + SEMs and are representative of two independent experiments for *P. brevis* and three independent experiments for *B. fragilis*. In (A) and (B), *P* values were calculated using the Mann-Whitney-Wilcoxon *U* test on parts per million (PPM) relative abundances for that feature in samples for pairwise comparisons. The combined *P* value (c*P*) for meta-analysis of group comparisons was calculated using Fishers *P* value. For each feature type, the cut-offs for the meta-analysis were: $P < 0.2$; $cP < 0.1$; false discovery rate (FDR) < 0.15. Tumor growth profiles [(A), (C), and (D)] were compared using Bonferroni-corrected two-way ANOVA. ****$P < 0.0001$; ns, not significant.

(Fig. 1C) or WT mice gavaged with $Gc^{-/-}$ fecal matter (Fig. 2, D and E, and fig. S3, A and B), mice fed with a high-$VitD_3$ diet did not exhibit increased tumor resistance if rendered deficient in T and B cells, cDC1, or MyD88 (Fig. 3E). Further resembling $Gc^{-/-}$ mice, FTs from WT mice that were fed with a high-$VitD_3$ diet increased the therapeutic efficacy of anti–CTLA-4 and anti–PD-1 immune checkpoint blockade

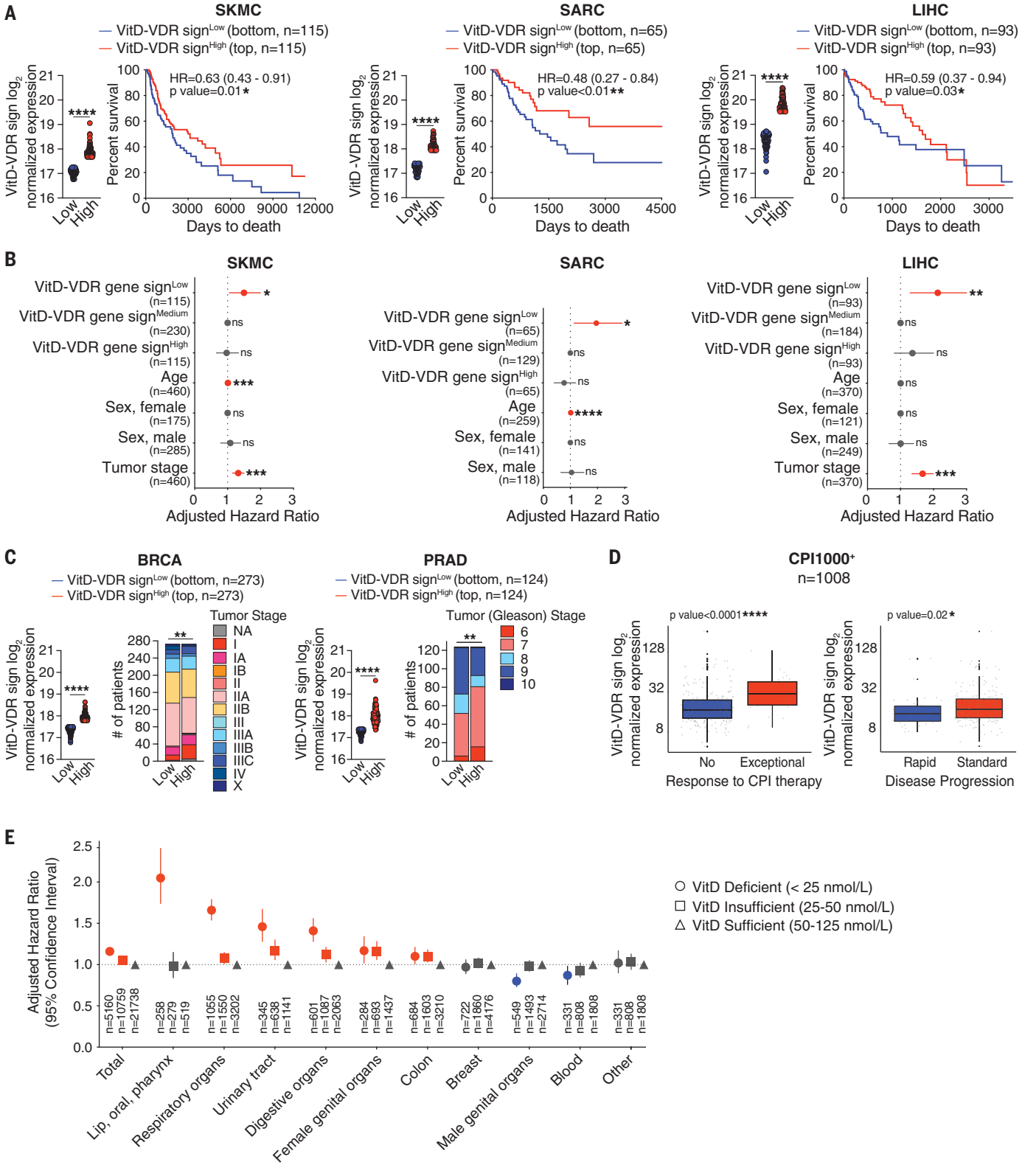

Fig. 6. VitD correlates with lower risk of cancer and increased patient survival. (**A**) Prognostic value of VitD-VDR gene signature levels for overall survival and HR comparing samples with the lowest (VitD-VDR sign^{Low}) versus highest (VitD-VDR sign^{High}) expression in the indicated TCGA datasets. Skin cutaneous melanoma (SKMC; *n* = 460), sarcoma (SARC; *n* = 259), liver hepatocellular carcinoma (LIHC; *n* = 370); bottom and top 25% of patient cohort. (**B**) HR, adjusted for age, sex, and tumor stage, comparing samples with the lowest (VitD-VDR sign^{Low}) or highest (VitD-VDR sign^{High}) versus medium (VitD-VDR sign^{Medium}) expression in the indicated TCGA datasets, as in (A). (**C**) Prognostic value of VitD-VDR signature levels for tumor stage comparing samples with the lowest (VitD-VDR sign^{Low}) versus highest (VitD-VDR = sign^{High}) expression in the indicated TCGA datasets. Breast cancer (BRCA; *n* = 1092),

prostate adenocarcinoma (PRAD; n = 497); bottom and top 25% of patient cohort. (**D**) VitD-VDR signature levels in samples with no response versus exceptional response (left) and rapid versus standard disease progression (right) of patients (n = 1008) treated with checkpoint inhibitors (CPI1000$^+$ cohort). (**E**) Estimated HR, adjusted for sex, age, and Charlson's comorbidity index, in the VitD deficient (<25 nmol/L) or insufficient (25 to 50 nmol/L) group versus the VitD sufficient (50 to 125 nmol/L) group of individuals (n = 1,496,766) that were living in Denmark between 2008 and 2017. In (A), data are presented as means of $\log_2$ normalized expressions ± SEMs. In (C), data are represented as number of patients that are subdivided on the basis of the tumor stage. In (D), data are presented as $\log_2$ normalized expression box-and-whisker plots with the median and 25th and 75th percentiles represented by the box and the min/max represented by the whiskers. Survival (Kaplan-Meier) curves in (A) were compared using log-rank (Mantel-Cox) test. In (A), (B), and (E), HRs with 95% confidence interval are shown. In (A) and (C), gene signature levels between groups were compared using two-tailed unpaired t test with Welch's correction. In (C), frequency of tumor stage was compared between groups using a Chi-squared test. In (D), expression of gene signature between the groups was compared using Wilcoxon signed-rank test. *P < 0.05; **P < 0.01; ***P < 0.001; ****P < 0.0001; ns, not significant.

inhibitors in transplantable cancer models other than 5555 Braf^{V600E} melanoma, such as MCA-205 and MC38 (Fig. 3, F to H). Collectively, these results establish that (i) high VitD levels favor a mouse microbiome that augments anticancer immunity and (ii) the favorable effect can be transferred by FT as long as VitD remains available to the recipient mice.

Increased vitamin D levels in mice favor a microbiome that potentiates cancer immunity

The fact that *Rag1*$^{-/-}$, *Batf3*$^{-/-}$, or *Myd88*$^{-/-}$ mice did not display VitD-driven increased immune resistance to cancer (Fig. 3E) was not because immune defects in those mice compromised the ability of a high-VitD_3 diet to promote favorable alterations in the microbiota. Fecal matter from all of the immunodeficient mice given high-VitD_3 diets was able to induce greater tumor resistance upon FT into WT mice (Fig. 4A). These data suggest that the ability of high VitD availability to alter the microbiome is largely independent of the immune system. To look for a nonimmune component, we turned our attention to the possible effects of VitD on IECs. Although it did not alter gut permeability (fig. S1E), a high-VitD_3 diet induced profound changes in gene expression in the colonic tissue of WT mice (fig. S5A). Gene expression analysis did not reveal marked compositional differences in specific immune cell populations, as predicted, but alterations were revealed in cellular signaling, cell junction organization, and defense from microbes (fig. S5, B to D). This is consistent with the ability of VitD, acting through VDR, to directly regulate the expression of multiple genes that affect host physiology (*22*, *34*). To directly assess the importance of VDR in IECs, we bred *Vdr*$^{fl/fl}$ mice to *Villin*^{Cre} mice to generate a *Vdr*$^{\Delta IEC}$ strain that lacks VDR expression in IECs (Fig. 4B). Upon weaning, VDR$^{\Delta IEC}$ mice were maintained on diets complemented with calcium, phosphorus, and lactose to mitigate the osteomalacia-like effects of abrogating VitD responsiveness in the gut epithelium (*35*). This altered diet did not prevent the ability of VitD_3 supplementation to increase tumor resistance in control WT mice [Fig. 4C; VitD_3 high$^+$ diet (where the + symbol denotes calcium/phosphorus/lactose complementation)]. However, the VitD_3 high$^+$ diet failed to increase tumor resistance in littermate VDR$^{\Delta IEC}$ mice (Fig. 4C). Furthermore, the fecal matter of VDR$^{\Delta IEC}$ mice on the VitD_3 high$^+$ diet was no longer able to transmit tumor resistance, unlike that of control WT littermates (Fig. 4D). These data indicate that VitD acts through IECs to favor a gut microbiome that increases immune-mediated cancer control.

To look for VitD-associated alterations in the microbiome, we carried out shotgun metagenomic analyses of fecal samples from mice in which we altered VitD levels by manipulating diet and/or genotype. We found that bacterial species alpha diversity was largely similar across all samples, whereas beta diversity and taxonomic profiles showed major differences across genotype but not diet (fig. S6, A to D; fig. S7, A and B; and fig. S8, A and B). To gain further insight into bacterial species modulated by VitD availability, we combined three meta-analyses of different comparisons across experiments: Meta1, differences driven by genotype (WT versus *Gc*$^{-/-}$) in a Vit$D_3^{Standard}$ condition; Meta2, differences driven by genotype (WT versus *Gc*$^{-/-}$) in the presence of varying levels of dietary VitD (Vit$D_3^{Standard}$ and VitD_3^{High}); and Meta3, differences driven by genotype (WT versus *Gc*$^{-/-}$) consistent with those driven by increased dietary VitD in WT (Vit$D_3^{Standard}$ versus VitD_3^{High}). This approach allowed us to identify 62 gene products and two taxa that were consistently regulated by VitD availability across conditions (Fig. 5, A and B, and fig. S9, A to C). Higher VitD availability increased the abundance of *B. fragilis* at the expense of *Prevotella brevis* (Fig. 5B; fig. S9, A to C; and fig. S10, A and B). Because the ability of *Gc*$^{-/-}$ mice to transmit tumor resistance through microbiota depends on the presence of dietary VitD, we removed background differences driven by genotype by contrasting *Gc*$^{-/-}$ and WT in mice fed Vit$D_3^{Deficient}$ and Vit$D_3^{Standard}$ diets and focused on taxonomic differences observed exclusively in the presence of VitD (Vit$D_3^{Standard}$). This analysis further confirmed the VitD-dependent increase in *B. fragilis* and reduction of *P. brevis* (fig. S10C). Therefore, we assessed whether either bacterium could affect tumor resistance in a VitD-dependent manner. Notably, three rounds of oral gavage with *B. fragilis* was sufficient to induce increased resistance to subsequent tumor transplantation across WT C576BL/6 mice procured from different sources and housed in two different animal units (Fig. 5C, left, and fig. S10D). However, and in line with our earlier data using FT (Fig. 3D), tumor resistance induced by *B. fragilis* was prevented if the recipient mice were placed on a diet deficient in VitD_3 (Fig. 5C, right). Thus, VitD availability is necessary to maintain a niche in which *B. fragilis* can thrive. Consistent with that notion, gavage with the bacterium led to slightly lower levels of the organism in the intestine of mice placed on a VitD_3-deficient diet compared with those on a VitD_3-standard diet (fig. S10E). In contrast to *B. fragilis*, gavage with *P. brevis* did not increase tumor resistance (Fig. 5C) and, in fact, decreased it slightly in mice placed on a VitD_3-deficient diet (Fig. 5C, right, and fig. S10F).

Vitamin D levels in humans correlate with cancer resistance

Polymorphisms in genes that encode proteins that participate in 1,25-$(OH)_2$D biosynthesis (*CYP2R1*, *CYP27A1*, and *CYP27B1*), that restrict VitD availability (*GC*), or that mediate VitD biological functions (*VDR*) have been variously correlated with cancer risk, alterations in microbiota, and/or changes in immune parameters in health and disease (*36*–*40*) (https://www.ebi.ac.uk/gwas/; fig. S11A and table S1). *VDR* is a ubiquitously expressed (fig. S11B) nuclear receptor that functions as a ligand-activated transcription factor. We therefore hypothesized that the expression of VDR target genes in any tissue, healthy or malignant, may act as a surrogate measurement of VitD availability in that tissue (*24*, *41*). We assembled a gene signature (VitD-VDR sign) consisting of 237 VDR target genes from several human cell types identified using chromatin immunoprecipitation assays with sequencing (ChIP-seq) datasets (table S2) (*11*, *42*–*46*). We confined our analysis to ChIP-seq data to increase resolution and ensure that we analyzed only primary VDR targets, even if this might exclude other relevant VitD-inducible genes. We examined the expression of the VitD-VDR sign in different cancers using data from The Cancer Genome Atlas (TCGA) collection (table S2). Analysis of skin cancer (n = 460 cases), sarcoma (n = 259), liver hepatocellular carcinoma (n = 370), breast cancer (n = 1092), and prostate adenocarcinoma (n = 497) revealed that lower

expression of the VitD-VDR signature correlated with poorer survival or more-advanced disease (Fig. 6, A to C). In the same cancers, the *VDR* transcript did not correlate with patient survival, highlighting a specific association of VDR target genes—but not necessarily *VDR* expression—with cancer progression (fig. S11, C and D). Comparison of human tumors with high versus low VitD-VDR sign revealed that VitD-VDR sign^{high} cancers displayed specific enrichment for genes and gene signatures of the same immune elements that we found to be required to restrict growth of mouse tumors after increased VitD availability (fig. S11E). This correlation between high VitD-VDR signature and gene signatures of antitumor immunity prompted us to further test the value of VitD-VDR sign in predicting responses to immunotherapy. We analyzed >1000 patients treated with immune checkpoint inhibitors (CPI1000^{+} cohort) across seven cancer types using bioinformatic pipelines and standardized clinical criteria, as reported (*47*). Low expression of VitD-VDR sign and, to a lesser extent, of *VDR* was associated with resistance to immune checkpoint inhibitors and more rapid disease progression (Fig. 6D and fig. S11F). Overall, these data suggest that, in humans as in mice, lower VitD tissue availability is associated with lower overall immune-mediated control and worse cancer outcome.

Several human epidemiological studies have associated high total (bound and unbound to Gc) and free VitD serum levels with decreased cancer onset and extended patient survival (*12*–*21*). However, these studies are inconclusive and limited by relatively small sample sizes. Therefore, we analyzed combined data from the Danish Central Person Registry, the Cancer Registry, and the Register of Laboratory Results for Research to include clinical information from a very large cohort of participants (1,496,766 individuals) that lived in Denmark and had at least one vitamin D (25-OHD) serum measurement registered between 2008 and 2017 (*48*, *49*) (Fig. 6E). Time elapsed since 1 year after first 25-OHD serum measurement until first diagnosis of cancer was analyzed by a Cox regression model using age as the underlying timescale and adjusting for sex, sample collection time, and Charlson's comorbidity index calculated on the 5 years before the sample was taken, as previously described (*50*). Skin pigmentation, which can affect $VitD_3$ production in response to sun exposure, was not available as a variable, but the analysis is unlikely to be affected by differences in ethnicity because the Danish population is highly homogeneous (86% of Danish descent). Further, the relatively northerly latitude of Denmark means that most of the year is a "vitamin D winter"—i.e., the period during which cutaneous synthesis of vitamin D_3 does not occur. Skin cancer was excluded from the study because sun exposure is a major confounder as it contributes to both $VitD_3$ synthesis and skin carcinogenesis. [In the previous analysis of cancer outcomes (Fig. 6, A, B, and D), this confounder is not relevant because we correlated VitD-induced transcripts with the outcome of patients that already developed skin cancer.] Notably, and consistent with our preclinical mouse models, we found that a low serum measurement of 25-OHD, indicative of vitamin D deficiency at the time the sample was taken, is associated with increased cancer risk in 6/10 individual cancer cohorts over the following decade. This analysis highlights that low vitamin D serum levels can be a prospective risk factor for cancer development in humans (Fig. 6E).

Discussion

The interplay between diet, microbiome, and the immune system is increasingly recognized as an important component of immunity, including to cancer (*51*–*53*). Studies in mice and humans have shown that gut commensals influence anticancer immune responses and affect the efficacy of immune checkpoint blockade therapy (*54*–*60*). The host factors that allow gut-resident microbes to modulate anticancer immune responses remain elusive. In this work, we show that increased VitD availability upon genetic deletion of Gc or after vitamin D dietary supplementation alters the gut microbiome to enhance cancer immunity (see graphical summary in fig. S12, A and B). Specifically, VitD levels appear to regulate the abundance and/or metabolic properties of *B. fragilis*, an anaerobic Gram-negative bacterium that is part of the normal microbiome of humans and mice. Notably, gavage of WT mice with fecal matter from $Gc^{-/-}$ mice or a nonenterotoxic clinical isolate of *B. fragilis* was sufficient to confer increased immune-mediated tumor resistance. This did not require antibiotic-mediated conditioning of the recipient mice but necessitated continued availability of dietary vitamin D, demonstrating the dependence of the putative *B. fragilis* niche on the micronutrient. Our data further indicate that this niche requires the activity of VitD on IECs, but further work will be required to understand which VDR-dependent IEC-derived factors are involved and whether they allow for *B. fragilis* expansion or alter its immunomodulatory activity. With regards to the latter, we do not presently know how *B. fragilis* acts to boost cancer immunity, although our findings suggest that MyD88-dependent receptor signaling and type I IFN production are necessary, as are cDC1-dependent T cell responses. *B. fragilis* has previously been associated with favorable antitumor immune responses after treatment of patients with anti–CTLA-4, whereas gut-resident *Prevotella* species had the opposite effect (*55*, *61*). Further, vitamin D supplementation in healthy human volunteers is associated with an increase in intestinal *Bacteroides* species and in the *Bacteroides*/*Prevotella* ratio (*62*, *63*), and abundance of *B. fragilis* in human infant fecal samples shows a positive correlation with maternal plasma 25-OHD levels (*64*). Thus, our data suggest a model in which VitD levels in humans, as in mice, modulate the ability of intestinal cells to produce mediators that select for an altered microbiome that includes organisms, such as *B. fragilis*, which potentiate cancer immunity (see graphical summary in fig. S12C). Whether this comes at the risk of adverse effects, especially given the ability of *B. fragilis* to become pathogenic (*65*), will require further assessment. However, in mice, we do not see evidence for *B. fragilis*–associated exacerbation of gut inflammation, and the bacterium is also reported to protect gut integrity and reduce colorectal cancer induction (*66*, *67*).

In some but not all studies, higher blood levels or increased dietary intake of vitamin D have been correlated with a lower risk of colorectal, breast, prostate, and pancreatic tumors (*12*–*21*). Our data from nearly 1.5 million individuals, the largest ever such cohort, confirm that a low VitD measurement correlates with increased subsequent risk of cancer incidence. Notably, this may be an underestimate of the true effect of VitD in cancer protection because those individuals who were found to be VitD deficient may have subsequently redressed it with dietary supplements, a factor that is not considered in our analysis. Notably, VitD levels at diagnosis of melanoma have been reported to positively correlate with both thinner tumors and better survival (*68*). Because it is exceedingly difficult to control for diet and sunlight exposure, and because a single measurement of VitD may not reflect actual vitamin D availability, we derived a VitD-VDR gene signature as a surrogate of tissue VitD activity. We show that this VitD-VDR gene signature correlates with cancer patient survival, consistent with studies showing that VitD can decrease cancer cell proliferation, promote apoptosis, reduce angiogenesis (*7*–*9*), and dampen the protumorigenic activity of cancer-associated fibroblasts (*10*, *11*). We further show that the VitD-VDR gene signature correlates with signatures of anticancer immunity and with patient responses to immunotherapy. Similarly, VDR expression in melanoma correlates with immune score and increased patient survival, possibly because VDR signals help counteract immunosuppressive Wnt signaling (*69*). Notably, a recent study has reported that greater VitD levels at baseline or after dietary correction correlate with higher responsiveness to immune checkpoint blockade therapy in a cohort of advanced melanoma patients (*70*). Thus, in humans, as in mice, VitD activity appears to potentiate immune responses to cancer.

We report that disrupted vitamin D signaling in IECs alters the intestinal microbiome,

which in turns affects immunity to cancer in mice. Further, we show that the vitamin D status of human patients and VitD-VDR signatures within tumors affects cancer incidence, survival, and/or the response to immunotherapy. Further work will be necessary to assess to what extent there is overlap between these two findings. Longitudinal studies in humans will help to disentangle the interaction between VitD availability with the microbiome and immunity to cancer as well as to better assess the effects of vitamin D dietary supplementation.

REFERENCES AND NOTES

1. E. A. Yamamoto, T. N. Jørgensen, *Front. Immunol.* **10**, 3141 (2020).
2. M. Medrano, E. Carrillo-Cruz, I. Montero, J. A. Perez-Simon, *Int. J. Mol. Sci.* **19**, 2663 (2018).
3. R. M. Lucas, S. Gorman, S. Geldenhuys, P. H. Hart, *F1000Prime Rep.* **6**, 118 (2014).
4. A. Clark, N. Mach, *Front. Immunol.* **7**, 627 (2016).
5. M. Waterhouse *et al*., *Eur. J. Nutr.* **58**, 2895–2910 (2019).
6. J. Wang *et al*., *Nat. Genet.* **48**, 1396–1406 (2016).
7. K. K. Deeb, D. L. Trump, C. S. Johnson, *Nat. Rev. Cancer* **7**, 684–700 (2007).
8. S.-M. Jeon, E.-A. Shin, *Exp. Mol. Med.* **50**, 1–14 (2018).
9. C. Carlberg, A. Muñoz, *Semin. Cancer Biol.* **79**, 217–230 (2022).
10. M. H. Sherman *et al*., *Cell* **159**, 80–93 (2014).
11. G. Ferrer-Mayorga *et al*., *Gut* **66**, 1449–1462 (2017).
12. J. Wactawski-Wende *et al*., *N. Engl. J. Med.* **354**, 684–696 (2006).
13. M. Jenab *et al*., *BMJ* **340**, b5500 (2010).
14. C. G. Woolcott *et al*., *Cancer Epidemiol. Biomarkers Prev.* **19**, 130–134 (2010).
15. S. Gandini *et al*., *Int. J. Cancer* **128**, 1414–1424 (2011).
16. Y. Ma *et al*., *J. Clin. Oncol.* **29**, 3775–3782 (2011).
17. J. De Smedt *et al*., *BMC Cancer* **17**, 562 (2017).
18. L. Yang, H. Chen, M. Zhao, P. Peng, *Oncotarget* **8**, 40214–40221 (2017).
19. J. E. Manson *et al*., *N. Engl. J. Med.* **380**, 33–44 (2019).
20. K. Ng *et al*., *JAMA* **321**, 1370–1379 (2019).
21. M. Urashima *et al*., *JAMA* **321**, 1361–1369 (2019).
22. D. D. Bikle, *Chem. Biol.* **21**, 319–329 (2014).
23. J. G. Haddad *et al*., *Biochemistry* **31**, 7174–7181 (1992).
24. F. F. Safadi *et al*., *J. Clin. Invest.* **103**, 239–251 (1999).
25. E. G. Duchow, N. E. Cooke, J. Seeman, L. A. Plum, H. F. DeLuca, *Proc. Natl. Acad. Sci. U.S.A.* **116**, 24527–24532 (2019).
26. C. M. Henderson *et al*., *N. Engl. J. Med.* **380**, 1150–1157 (2019).
27. J. P. Böttcher, C. Reis e Sousa, *Trends Cancer* **4**, 784–792 (2018).
28. S. K. Wculek *et al*., *Nat. Rev. Immunol.* **20**, 7–24 (2020).
29. J. Canton *et al*., *Nat. Immunol.* **22**, 140–153 (2021).
30. C. M. Henry, C. A. Castellanos, C. Reis e Sousa, *Semin. Immunol.* **66**, 101726 (2023).
31. E. Giampazolias *et al*., *Cell* **184**, 4016–4031.e22 (2021).
32. K. H. J. Lim *et al*., *J. Immunother. Cancer* **10**, e005245 (2022).
33. W. M. Lee, R. M. Galbraith, *N. Engl. J. Med.* **326**, 1335–1341 (1992).
34. O. Koivisto, A. Hanel, C. Carlberg, *Nutrients* **12**, 1140 (2020).
35. M. Amling *et al*., *Endocrinology* **140**, 4982–4987 (1999).
36. A. M. Mondul *et al*., *Cancer Epidemiol. Biomarkers Prev.* **22**, 688–696 (2013).
37. L. Zhou *et al*., *Int. J. Clin. Exp. Med.* **5**, 72–79 (2012).
38. S. Karami *et al*., *Cancer Epidemiol. Biomarkers Prev.* **22**, 1557–1566 (2013).
39. M. Peña-Chilet *et al*., *PLOS ONE* **8**, e59607 (2013).
40. L. N. Anderson, M. Cotterchio, D. E. C. Cole, J. A. Knight, *Cancer Epidemiol. Biomarkers Prev.* **20**, 1708–1717 (2011).
41. R. F. Chun, *Cell Biochem. Funct.* **30**, 445–456 (2012).
42. S. V. Ramagopalan *et al*., *Genome Res.* **20**, 1352–1360 (2010).
43. N. Ding *et al*., *Cell* **153**, 601–613 (2013).
44. V. Nurminen, S. Seuter, C. Carlberg, *Front. Physiol.* **10**, 194 (2019).
45. M. Kawai *et al*., *JCI Insight* **4**, e121798 (2019).
46. A. Hanel *et al*., *Sci. Rep.* **10**, 21051 (2020).
47. K. Litchfield *et al*., *Cell* **184**, 596–614.e14 (2021).
48. M. L. Gjerstorff, *Scand. J. Public Health* **39**, 42–45 (2011).
49. J. F. H. Arendt *et al*., *Clin. Epidemiol.* **12**, 469–475 (2020).
50. H. Quan *et al*., *Med. Care* **43**, 1130–1139 (2005).
51. C.-B. Zhou, Y.-L. Zhou, J.-Y. Fang, *Trends Cancer* **7**, 647–660 (2021).
52. C. Villemin *et al*., *Trends Immunol.* **44**, 44–59 (2023).
53. M. Alexander, P. J. Turnbaugh, *Immunity* **53**, 264–276 (2020).
54. A. Sivan *et al*., *Science* **350**, 1084–1089 (2015).
55. M. Vétizou *et al*., *Science* **350**, 1079–1084 (2015).
56. B. Routy *et al*., *Science* **359**, 91–97 (2018).
57. T. Tanoue *et al*., *Nature* **565**, 600–605 (2019).
58. V. Gopalakrishnan *et al*., *Science* **359**, 97–103 (2018).
59. L. F. Mager *et al*., *Science* **369**, 1481–1489 (2020).
60. K. C. Lam *et al*., *Cell* **184**, 5338–5356.e21 (2021).
61. C.-H. Lo *et al*., *J. Biomed. Sci.* **29**, 88 (2022).
62. N. Charoenngam, A. Shirvani, T. A. Kalajian, A. Song, M. F. Holick, *Anticancer Res.* **40**, 551–556 (2020).
63. P. Singh, A. Rawat, M. Alwakeel, E. Sharif, S. Al Khodor, *Sci. Rep.* **10**, 21641 (2020).
64. C. E. Talsness *et al*., *PLOS ONE* **12**, e0188011 (2017).
65. S. Patrick, *Microbiology* **168**, 001156 (2022).
66. M. H. Sofi *et al*., *JCI Insight* **6**, e136841 (2021).
67. Y. K. Lee *et al*., *MSphere* **3**, e00587-18 (2018).
68. J. A. Newton-Bishop *et al*., *J. Clin. Oncol.* **27**, 5439–5444 (2009).
69. S. Muralidhar *et al*., *Cancer Res.* **79**, 5986–5998 (2019).
70. Ł. Galus *et al*., *Cancer* **129**, 2047–2055 (2023).

ACKNOWLEDGMENTS

We thank the members of the Immunobiology Laboratory for helpful discussions and suggestions. We thank G. Stockinger for reading an original draft of the manuscript and valuable input. We thank the Crick Science Technology Platforms, including Biological Research Facility, Flow Cytometry, Metabolomics, and Experimental Histopathology, as well as CRUK Manchester Institute Biological Resource Unit and the Frederick National Laboratory Gnotobiotics Facility (NCI, NIH) for their support throughout this project. **Funding:** This work was supported by The Francis Crick Institute, which receives core funding from Cancer Research UK (CC2090), the UK Medical Research Council (CC2090), and the Wellcome Trust (CC2090); an ERC Advanced Investigator grant (AdG 268670); a Wellcome Investigator award (106973/Z/15/Z); and a prize from the Louis-Jeantet Foundation. E.G. is currently supported by a Cancer Research UK Institute award (C5759/A27412) and a Royal Society research grant (RG\R2\232348). M.P.d.C. was supported by Boehringer Ingelheim Fonds. K.H.J.L. was supported by a Wellcome Imperial 4i Clinical Research Fellowship (216327/Z/19/Z). A.B. was supported by the Human Frontier Science Program postdoctoral fellowship (LT0061/2022) and an EMBO nonstipendiary long-term fellowship (ALTF 662-2021). M.A.K. and S.Z. were supported by a Cancer Research UK Institute award (DRCSGL-2023/100001). This research was funded in part by the Wellcome Trust (grants CC2090, 106973/Z/15/Z, and 216327/Z/19/Z). K.C.L., R.R.R., and R.S.G. are supported by the Intramural Research Program of the National Institutes of Health (CCR-NCI). K.R.P. and S.B. were supported by the ERC (grant no. 866028) and the UK Medical Research Council (project no. MC_UU_00025/11). J.C.L. is a Lister prize fellow. T.J. and G.J.P. were supported by the Danish National Research Foundation (DNRF148). **Author contributions:** E.G. conducted experiments and analyzed data with assistance from M.P.d.C., K.C.L., K.H.J.L., A.C., C.P., S.P., A.B., T.C.-D., M.D.B., M.A.K., P.W., and A.V. S.L. provided technical support. E.G. oversaw the research activity planning and execution that was performed by S.P., P.W., and A.V. S.Z. oversaw the research activity planning and execution that was performed by M.A.K. K.C.L. performed experiments on germ-free mice. R.S.G. oversaw the research activity planning and execution that was performed by K.C.L. T.J. and K.C.L. provided access to data and the metadata analysis pipeline for bioinformatic analysis. P.C., K.C.L., R.R.R., G.J.P., B.S., and E.G. carried out bioinformatic analyses. J.C.L. and R.S.G. helped with analysis and experimental design. C.M.M., E.C., C.P., and A.I. helped with the harvesting and processing of tissue and tumor samples. E.N., E.G., and B.F. processed and cut tissue for histological analysis. A.C., A.S.-B., and S.L.P. conducted histopathology assessments blindly. S.B. and K.R.P. cultured *B. fragilis* and *P. brevis*. E.G., A.C., and S.O. performed fecal microbiota transplantations as well as *B. fragilis* and *P. brevis* oral administration. S.A.P.-D. and J.I.M. measured the vitamin D concentration in mouse serum. R.G. performed the RNA sequencing of mouse colons. N.C.R. managed the mouse colonies. E.G. and C.R.e.S. designed the study, interpreted data, and wrote the manuscript. All authors reviewed and edited the manuscript. **Competing interests:** C.R.e.S. is a founder of Adendra Therapeutics and owns stock options and/or is a paid consultant or advisory board member for Adendra Therapeutics, Montis Biosciences, and Bicycle Therapeutics, all unrelated to this work. C.R.e.S. has an additional appointment as a visiting professor in the Faculty of Medicine at Imperial College London and holds honorary professorships at University College London and King's College London. The authors declare no other competing interests. **Data and materials availability:** All data are available in the manuscript or the supplementary materials. Materials and reagents described in this study are either commercially available or available on request from the corresponding authors. Shotgun metagenomics data are available through the National Center for Biotechnology Information Sequence Read Archive (NCBI SRA) under BioProject ID PRJNA1077927. Colon RNA sequencing data have been deposited in the Gene Expression Omnibus (GEO) database under the accession no. GSE219214.

SUPPLEMENTARY MATERIALS

science.org/doi/10.1126/science.adh7954
Materials and Methods
Figs. S1 to S12
Tables S1 to S3
References (*71–80*)
MDAR Reproducibility Checklist

Submitted 14 March 2023; resubmitted 2 December 2023
Accepted 4 March 2024
10.1126/science.adh7954